Vibrational Modes of the Protonated Schiff Base in *pharaonis* Phoborhodopsin†

Kazumi Shimono,‡ Yuji Furutani,§,||,⊥ Naoki Kamo,‡ and Hideki Kandori*,§,⊥

Laboratory of Biophysical Chemistry, Graduate School of Pharmaceutical Sciences, Hokkaido University, Sapporo 060-0812, Japan, Department of Applied Chemistry, Nagoya Institute of Technology, Showa-ku, Nagoya 466-8555, Japan, Department of Biophysics, Graduate School of Science, Kyoto University, Sakyo-ku, Kyoto 606-8502, Japan, and Core Research for Evolutional Science and Technology (CREST), Japan Science and Technology Corporation, Kyoto 606-8502, Japan

Received February 19, 2003; Revised Manuscript Received April 20, 2003

ABSTRACT: *pharaonis* phoborhodopsin (*p*pR; also called *pharaonis* sensory rhodopsin II, *p*sR-II) is a photoreceptor for negative phototaxis in *Natronobacterium pharaonis*. Recent X-ray crystallographic structures showed that *p*pR and bacteriorhodopsin (BR), a light-driven proton pump, possess similar molecular environments of the retinal Schiff base. Nevertheless, absorption spectra are different by 70 nm between *p*pR and BR, suggesting the different chromophore−protein interactions involving the Schiff base region. In this article, we identify frequencies of the Schiff base vibrations in the ppR$_K$ minus *p*pR difference spectra by means of low-temperature FTIR spectroscopy of [ζ-^{15}N]lysine-labeled *p*pR. The N−D stretch in D_2O was found at 2140 and 2091 cm^{-1} for *p*pR, which are shifted to a lower frequency by 32−33 cm^{-1} compared to those for BR. This observation indicates the stronger hydrogen bond of the Schiff base in *p*pR than in BR. The N−D stretch of the Schiff base and O−D stretch of water molecules are located at the different frequencies in *p*pR, while they appear in the same frequency region in BR [Kandori, H., Belenky, M., and Herzfeld, J. (2002) *Biochemistry 41,* 6026−6031]. These differences could be correlated with the distorted pentagonal cluster structure in *p*pR. In contrast, the N−D stretch of ppR$_K$ was found at 2474 cm^{-1}, which is close in frequency to that of BR$_K$. The O−D stretch of Thr79 was also assigned at 2512 and 2474 cm^{-1} for *p*pR and ppR$_K$, respectively. These frequencies are close to those of BR, suggesting the interaction of Thr79 and Asp75 in *p*pR is similar to that of Thr89 and Asp85 in BR.

pharaonis phoborhodopsin (*p*pR)[1] from *Natronobacterium pharaonis* is a member of the archaeal rhodopsins (*1*, *2*). *p*pR activates a cognate transducer protein upon light absorption, leading to negative phototaxis. It possesses a retinal chromophore that is embedded within seven-transmembrane helices, like the well-studied proton-pump protein bacteriorhodopsin (BR) (*1*−*3*). In *p*pR or BR, the retinal forms a Schiff base linkage with Lys205 or Lys216, respectively, and the protonated Schiff base is stabilized by a negatively charged counterion, Asp75 or Asp85, respectively. Light absorption of *p*pR triggers trans−cis photoisomerization of the retinal chromophore in its electronically excited state (*4*), followed by rapid formation of the ground-state species such as the K intermediate (*5*). This process is also the case in BR. Relaxation of the primary intermediates eventually leads to functional processes during their photocycles (*1*−*3*).

A recently determined crystal structure of *p*pR showed surprisingly similar architectures between *p*pR and BR (*6*, *7*). Thus, the functional difference is presumably due to the fine structural variants between them. Figure 1 shows the Schiff base region of *p*pR [PDB entry 1H68 (*7*)]. There are three water molecules in this region, forming a pentagonal cluster structure with carboxylic oxygens of Asp75 and Asp201. Water402 bridges the Schiff base and Asp75, where Asp201 is also located within hydrogen bonding distance. Thr79 forms a hydrogen bond with another carboxylic oxygen of Asp75. These structural features are common in BR (*8*). Nevertheless, there are certain differences between *p*pR and BR. First, the pentagonal cluster structure is considerably distorted in *p*pR. The five hydrogen bonding distances within the pentagonal cluster are 2.5−3.1 Å (Figure 1) and 2.6−2.8 Å in *p*pR and BR, respectively, and the pentagonal cluster is less planer in *p*pR than in BR (*8*). Second, the direction of the side chain of Arg72 in *p*pR differs from that in BR (Arg82), and Arg72 does not form a hydrogen bond with the pentagonal cluster. This may be one of the reasons that *p*pR has the distorted pentagonal cluster structure. The distorted pentagonal cluster structure in *p*pR could be related to the difference in color and function between *p*pR and BR.

Vibrational analysis is a powerful tool for investigation of hydrogen bonds. In particular, the O−H and N−H (O−D and N−D) stretching modes are direct probes of hydrogen bond strength. By means of low-temperature polarized FTIR

† This work was supported by grants from the Japanese Ministry of Education, Culture, Sports, Science, and Technology to H.K. and by Research Fellowships from the Japan Society for the Promotion of Science for Young Scientists to K.S. and Y.F.

* To whom correspondence should be addressed. Phone and Fax: 81-52-735-5207. E-mail: kandori@ach.nitech.ac.jp.

‡ Hokkaido University.

§ Nagoya Institute of Technology.

|| Kyoto University.

⊥ CREST.

[1] Abbreviations: *p*pR, *pharaonis* phoborhodopsin; ppR$_K$, K intermediate of *p*pR; BR, light-adapted bacteriorhodopsin that has all-trans-retinal as its chromophore; BR$_K$, K intermediate of BR; FTIR, Fourier transform infrared.

10.1021/bi034284m CCC: $25.00
Published on Web 05/28/2003

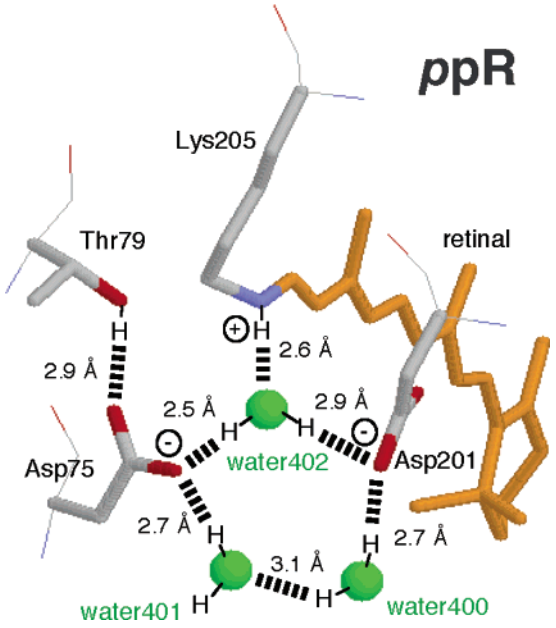

FIGURE 1: Diffraction structure of the Schiff base region in *p*pR from PDB entry 1H68 (*7*). The membrane normal is approximately in the vertical plane. Upper and lower regions correspond to the cytoplasmic and extracellular sides, respectively. Green circles (400−402) represent water molecules which form a distorted pentagonal cluster with an oxygen from Asp75 and an oxygen from Asp201. This structure is very similar to that by another group, where water400 is called water406 (*6*).

spectroscopy with oriented BR, we have assigned vibrational modes in the Schiff base region, such as internal water molecules (*9*−*11*), the N−D stretch of the Schiff base (*12*), and the O−D stretch of Thr89 (*13*−*15*). These results provided useful information about the hydrogen bonding alterations in the BR function. Therefore, comparative IR investigation of vibrations in the Schiff base region between *p*pR and BR is important in understanding each mechanism in atomic detail.

In 2001, we reported the *p*pR$_K$ minus *p*pR difference spectra in the whole mid-infrared region (*16*), which allowed the spectral comparison with those of BR. The BR$_K$ minus BR spectrum in D_2O exhibits a strong negative peak at 2171 cm^{-1}, which contains both the N−D stretch of the Schiff base and the O−D stretch of water (*8*−*12*). The *p*pR$_K$ minus *p*pR spectrum in D_2O similarly exhibits a strong negative peak at 2090 cm^{-1} (*16*). Nevertheless, spectral analysis in D_2O and $D_2{}^{18}O$ revealed that the 2090 cm^{-1} band does not contain the O−D stretch of water molecules. Water O−D stretches of *p*pR were identified at 2307 and 2215 cm^{-1} (*16*), which are higher in frequency than those of BR at 2292 and 2171 cm^{-1} (*10*). These observations were interpreted in connection with the distorted pentagonal cluster structure in *p*pR (*8*). In this way, water bands have been well-characterized, whereas the 2090 cm^{-1} band of *p*pR remained unidentified.

In the study presented here, we attempted to assign the N−D stretching vibration of the protonated Schiff base in *p*pR and its K intermediate. To this end, low-temperature FTIR spectroscopy was applied to hydrated films of [ζ-^{15}N]-lysine-labeled and unlabeled *p*pR in D_2O. Highly accurate comparative study eventually led to identification of the frequency of the N−D stretching vibrations of the Schiff base, as well as the C═N stretches in *p*pR and *p*pR$_K$. In addition, the O−D stretches of Thr79 are assigned by use of the mutant proteins of Thr79. Structure and structural changes of the local environment of the Schiff base are discussed in light of these results.

MATERIALS AND METHODS

[ζ-^{15}N]Lysine-labeled and unlabeled *p*pR with a histidine tag at the C-terminus were expressed in *Escherichia coli* strain BL21(DE3) (Invitrogen), and were grown in M9 medium.[2] Labeled and unlabeled L-lysine (50 mg/L) (Isotech) were added to the medium 1 h before induction by the addition of 1 mM IPTG and 10 μM all-trans-retinal (*17*, *18*). [ζ-^{15}N]Lysine-labeled and unlabeled *p*pR were solubilized with 1.5% *n*-dodecyl β-D-maltoside, followed by purification with Ni−NTA agarose (Qiagen) as described previously (*19*). We reconstituted the purified sample into L-α-phosphatidylcholine (PC, egg, Avanti) liposomes by gently stirring with detergent-adsorbing biobeads (100 mg of biobeads/mg of protein; Bio-Rad) for 12 h at room temperature. The molar ratio of added PC was 50 times that of *p*pR. After removal of the biobeads by filtration, the reconstitution protein was pelleted by centrifugation at 15000*g* for 30 min at 4 °C and washed twice with 10 mM phosphate buffer (pH 7) containing 200 mM NaCl (*20*, *21*).

FTIR spectroscopy was applied as described previously (*16*, *19*, *22*). The *p*pR sample in the PC liposome was washed twice with a buffer [2 mM phosphate (pH 7)]. A 90 μL portion of the *p*pR sample was dried on a BaF_2 window with a diameter of 18 mm. After hydration by either H_2O or D_2O, the sample was placed in a cell, which was mounted in an Oxford DN-1704 cryostat in the Bio-Rad FTS-40 spectrometer. Illumination conditions for *p*pR were identical to those reported previously: 450 nm light for the *p*pR to *p*pR$_K$ conversion and >560 nm light for the *p*pR$_K$ to *p*pR reversion at 77 K (*16*, *19*). The difference spectrum was calculated from the spectra constructed with 128 interferograms before and after the illumination. Twenty-four spectra obtained in this way were averaged for the *p*pR$_K$ minus *p*pR spectrum.

RESULTS

Assignment of the C═N Stretching Vibration of the Protonated Schiff Base in ppR and Its K Photointermediate. In this study, we prepared the [ζ-^{15}N]Lys-labeled *p*pR samples to assign the vibrational modes of the protonated Schiff base. It is noted that the ^{15}N labeling did not cause any substantial changes in other bands. Figure 2 shows the spectral changes in the frequency region of the C═N stretching mode of the retinal Schiff base. As is clearly seen, the intensities of broad negative bands at 1657 and 1651 cm^{-1} are reduced significantly in the [ζ-^{15}N]Lys-labeled *p*pR sample, while a new negative band appears at 1635 cm^{-1} (Figure 2a). The difference indicates the peak of the C═NH and C═^{15}NH stretches in *p*pR at 1657 and 1638 cm^{-1}, respectively (Figure 2b). Thus, we assigned the C═NH stretch of *p*pR to 1657 cm^{-1}. It is noted that the negative

[2] M9 minimum medium per liter: 7 g of $NaHPO_4$, 3 g of KH_2PO_4, 0.5 g of NaCl, 20 mg of thymidine, 20 mg of adenosine, 20 mg of guanosine, 20 mg of cytidine, 20 mg of thiamine, 20 mg of biotin, 0.33 mL of 10 mM $FeCl_3$, 0.12 g of $MgSO_4$, 10 mg of $MnCl_2{\cdot}4H_2O$, 4 g of glucose, 0.5 g of NH_4Cl, 1.5 mL of 75% glycerol, and 2 mL of 50 mM $CaCl_2$.

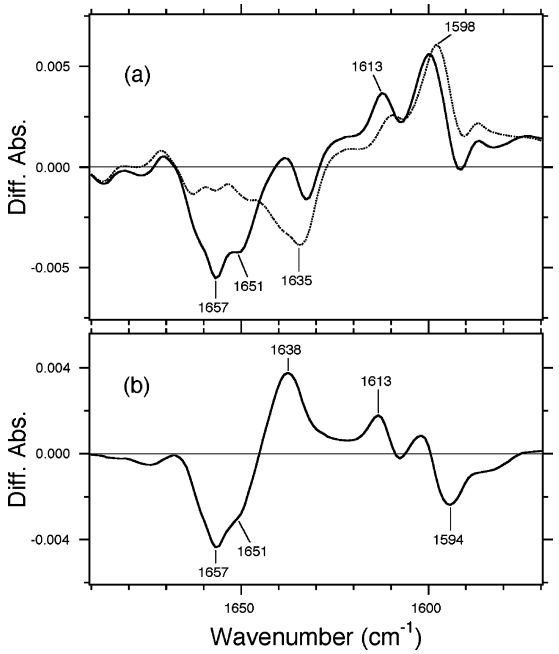

FIGURE 2: (a) ppR$_K$ minus ppR difference infrared spectra of unlabeled (—) and [ζ-^{15}N]Lys-labeled (···) ppR in the 1690−1570 cm^{-1} region. The sample was hydrated with H_2O, and spectra were measured at 77 K. (b) Difference spectrum between labeled and unlabeled samples, where the spectrum of labeled ppR is subtracted from that of unlabeled ppR in panel a.

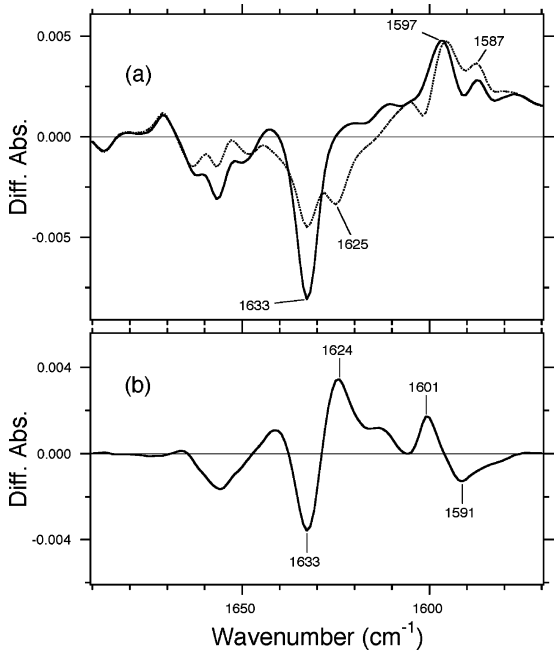

FIGURE 3: (a) ppR$_K$ minus ppR difference infrared spectra of unlabeled (—) and [ζ-^{15}N]Lys-labeled (···) ppR in the 1690−1570 cm^{-1} region. The sample was hydrated with D_2O, and spectra were measured at 77 K. (b) Difference spectrum between labeled and unlabeled samples, where the spectrum of labeled ppR is subtracted from that of unlabeled ppR in panel a.

peak in Figure 2b has a shoulder at 1651 cm^{-1}, which is also present in the ppR$_K$ minus ppR difference spectrum (solid line in panel a). This suggests the presence of another vibrational frequency for the C═NH stretch, possibly originating from the heterogeneous environment.

Upon formation of ppR$_K$, peaks appear in the 1630−1570 cm^{-1} region. Among them, the positive 1613 cm^{-1} band disappears in the [ζ-^{15}N]Lys-labeled ppR sample, which possesses a peak at 1598 cm^{-1} (Figure 2a). The difference indicates the peak of the C═NH and C═^{15}NH stretches in ppR$_K$ at 1613 and 1594 cm^{-1}, respectively (Figure 2b). Thus, we assigned the C═NH stretch of ppR$_K$ to 1613 cm^{-1}.

Figure 3 shows the same experiment as Figure 2 under conditions of D_2O hydration. The intensity of a sharp negative band at 1633 cm^{-1} is reduced by half in the [ζ-^{15}N]-Lys-labeled ppR sample, while a new negative band appears at 1625 cm^{-1} (Figure 3a). The difference indicates the peaks of the C═ND and C═^{15}ND stretches in ppR at 1633 and 1624 cm^{-1}, respectively (Figure 3b). Thus, we assigned the C═ND stretch of ppR to 1633 cm^{-1}.

Upon formation of ppR$_K$, a peak appears at 1597 cm^{-1} (solid line in Figure 3a), whose higher-frequency side reduces the intensity in the [ζ-^{15}N]Lys-labeled ppR sample (dotted line). On the other hand, the lower-frequency side increases the intensity. The difference indicates the peaks of the C═ND and C═^{15}ND stretches in ppR$_K$ at 1601 and 1591 cm^{-1}, respectively (Figure 3b). Thus, we assigned the C═ND stretch of ppR$_K$ to 1601 cm^{-1}.

From the isotope label of lysine, we assigned the C═NH and C═ND stretches of the Schiff base in ppR to 1657 and 1633 cm^{-1}, respectively. The difference of 24 cm^{-1} is close to that determined by resonance Raman spectroscopy (23 cm^{-1}) (*23*), and is larger than that of BR (13 cm^{-1}) (*19*). It is generally accepted that the spectral upshift in H_2O is caused by the coupling of the N−H bending vibration with the C═N stretch of the Schiff base, and the difference in frequency between H_2O and D_2O is the measure of the hydrogen bond strength of the Schiff base (*24*−*26*). Thus, the hydrogen bond of the Schiff base in ppR is stronger than in BR. We also assigned the C═NH and C═ND stretches of the Schiff base in ppR$_K$ to 1613 and 1601 cm^{-1}, respectively. The reduced difference (12 cm^{-1}) indicates a weakened hydrogen bond upon retinal photoisomerization.

Assignment of the N−D Stretching Vibration of the Protonated Schiff Base in ppR and Its K Photointermediate in D_2O. As described above, the hydrogen bond strength of the Schiff base is well evaluated by the difference between C═NH and C═ND stretching vibrations. Another and more direct probe of the hydrogen bond strength of the protonated Schiff base is the N−H stretching vibration. Its frequency is lowered when the hydrogen bond is strengthened, as are those of other N−H stretches. However, it is difficult to identify the N−H stretch in the difference infrared spectra, because a large number of N−H and O−H vibrations can mask it. We recently showed that in the case of BR, we are able to detect the N−D stretch, since the Schiff base proton is deuterated in D_2O. In BR, we assigned the N−D stretch of the Schiff base to 2173 and 2123 cm^{-1} (*12*). On the other hand, BR$_K$ possesses the N−D stretch at 2495 and 2468 cm^{-1} (*12*). A higher-frequency shift of ∼300 cm^{-1} indicates a significantly weakened hydrogen bond of the protonated Schiff base after retinal photoisomerization. This observation is consistent with the analysis of the C═N stretch and crystallographic structures of BR$_K$ (*27*−*29*).

We attempted to use a similar approach to the ppR$_K$ minus ppR difference spectra. Figure 4 compares the X−D stretching frequency region between unlabeled (solid line) and [ζ-^{15}N]Lys-labeled (dotted line) ppR. The negative bands at 2140 and 2091 cm^{-1} are downshifted to 2137 and 2084 cm^{-1},

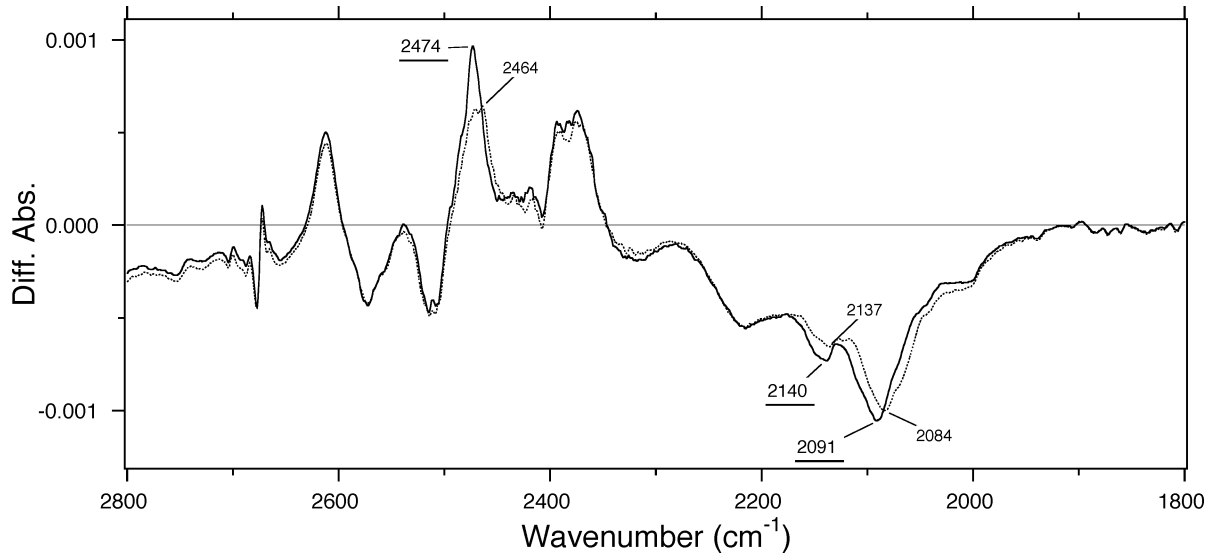

FIGURE 4: *p*pR$_K$ minus *p*pR difference infrared spectra of unlabeled (—) and [ζ-^{15}N]Lys-labeled (•••) *p*pR in the 1690−1570 cm^{-1} region. The sample was hydrated with D_2O, and spectra were measured at 77 K.

respectively, in [ζ-^{15}N]Lys-labeled BR, indicating that the band originates from the N−D stretching vibration of the Schiff base in *p*pR.[3] A previous comparison between spectra in D_2O and $D_2{}^{18}O$ indicated that the negative 2140 and 2091 cm^{-1} bands do not contain water O−D stretching vibrations, whereas the bands in the region of 2400−2200 cm^{-1} originate from water (*8*, *16*). Thus, in *p*pR, the Schiff base N−D stretch and water O−D stretches are split in frequency.

While the other frequency region shows well-overlapped spectra between unlabeled (solid line) and [ζ-^{15}N]Lys-labeled (dotted line) *p*pR, a clear spectral difference is visible at ∼2470 cm^{-1} (Figure 4). The positive band at 2474 cm^{-1} is downshifted to 2464 cm^{-1} in [ζ-^{15}N]Lys-labeled *p*pR, indicating that the band originates from the N−D stretching vibration of the Schiff base in *p*pR$_K$. Thus, the N−D stretch of the Schiff base is upshifted by 300−400 cm^{-1} upon retinal photoisomerization, indicating that the hydrogen bond of the Schiff base is significantly weakened. This observation is consistent with the analysis of the C═N stretch. The crystallographic structure of *p*pR$_K$ provided the same conclusion (*30*).

Assignment of the O−D Stretching Vibration of Thr79 in ppR and Its K Photointermediate in D_2O. It is known that the OH group of Thr89 in BR is deuterated in D_2O, and the O−D stretch appears at 2506 cm^{-1} (*13*−*15*). BR$_K$ has the O−D stretch at 2466 cm^{-1}, which also contains the N−D stretch of the Schiff base (*12*). Figure 5a shows this frequency region in Figure 4 expanded. The *p*pR$_K$ minus *p*pR spectrum has peaks at 2512 (−)/2474 (+) cm^{-1} (dotted line in Figure 5a), and only the positive band exhibits spectral downshift in [ζ-^{15}N]Lys-labeled *p*pR (solid line). This spectral feature is similar to that of BR (*12*), suggesting that the negative 2512 cm^{-1} band in *p*pR originates from the O−D stretch of Thr79 (Figure 1). In this study, we recorded the IR spectra of the mutant proteins of Thr79 to examine the O−D stretch of Thr79.

[3] We recently showed that complex formation of *p*pR with its transducer protein does not change the frequencies of the N−D stretch of the Schiff base and the O−D stretch of water molecules (*34*). The environment of the Schiff base is thus identical in the native complex state to that in *p*pR, the latter of which is studied here.

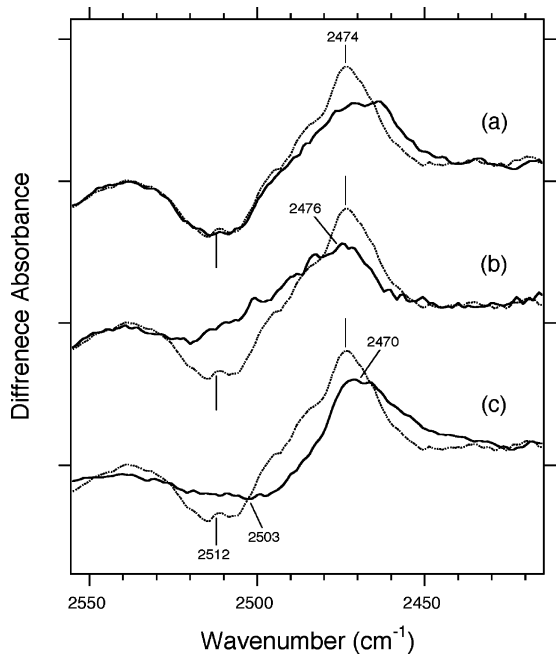

FIGURE 5: (a) *p*pR$_K$ minus *p*pR difference infrared spectra of unlabeled (•••) and [ζ-^{15}N]Lys-labeled (—) *p*pR in the 2555−2415 cm^{-1} region. The sample was hydrated with D_2O, and spectra were measured at 77 K. (b) *p*pR$_K$ minus *p*pR difference infrared spectra of the wild type (•••, same as in trace a) and the T79A mutant of *p*pR (—). (c) *p*pR$_K$ minus *p*pR difference infrared spectra of the wild type (•••, same as in trace a) and the T79S mutant of *p*pR (—). One division of the *Y*-axis corresponds to 0.001 absorbance unit.

Solid lines in parts b and c of Figure 5 represent the *p*pR$_K$ minus *p*pR spectra of T79A and T79S, respectively. Fingerprint vibrations (1250−1100 cm^{-1}) showed that the K intermediates were normally produced in T79A and T79S (data not shown). In the case of T79A, the negative 2512 cm^{-1} band disappears, while the positive band appears at 2476 cm^{-1} with a reduction in its intensity (Figure 5b). On the other hand, it appears that there is a broad negative band at ∼2503 cm^{-1} in T79S (Figure 5c). The positive peak (2470 cm^{-1}) in T79S is downshifted from that of wild-type *p*pR. These spectral features in *p*pR are similar to those of the mutants of Thr89 in BR. In fact, the negative 2506 cm^{-1}

band disappears in T89A, and is downshifted to 2481 cm^{-1} in T89S (*13*). An O−H (O−D) stretch of serine lower than that of threonine is common among BR (*13*, *15*), visual rhodopsin (*31*), and *p*pR. Thus, though we did not measure the level of the isotope label of threonine, this mutant analysis strongly suggests that the bands at 2512 (−) and 2474 (+) cm^{-1} originate from the O−D stretch of Thr79 in *p*pR and pR_K, respectively. In addition, the positive 2474 cm^{-1} band contains the N−D stretch of the protonated Schiff base of pR_K.

DISCUSSION

This FTIR study identified the frequencies of the Schiff base vibrations in *p*pR and pR_K at 77 K. The frequencies of the C═NH and C═ND stretches were found to be 1657 and 1633 cm^{-1}, respectively, for *p*pR and 1613 and 1601 cm^{-1}, respectively, for pR_K. On the other hand, the frequencies of the N−D stretch were found to be 2140 and 2091 cm^{-1} for *p*pR and 2474 cm^{-1} for pR_K. Frequencies in stretching vibrations are generally lowered when hydrogen bonds are strengthened. Therefore, the shift to a higher frequency upon K formation by 300−400 cm^{-1} indicates a weakened hydrogen bond accompanies photoisomerization. This observation is consistent with the vibrational analysis for the C═N stretching mode, where the difference in frequency between observations in H_2O and D_2O has been regarded as the measure of the hydrogen bond strength of the Schiff base (*24*−*26*).

The N−D stretches of *p*pR at 2140 and 2091 cm^{-1} are shifted to lower frequencies by 32−33 cm^{-1} compared to those for BR. This observation indicates that the hydrogen bond of the Schiff base is stronger in *p*pR than in BR. In contrast, the N−D stretch of pR_K was found at 2474 cm^{-1}, which is close in frequency to that of BR_K (*12*). These facts suggest that the ND group is not hydrogen bonded in the K state. The mechanism of photoisomerization, such as the direction of bond rotation and pointing of the ND group in the K state, etc., may be similar for *p*pR and BR.

The O−D stretch of Thr79 was also assigned to 2512 and 2474 cm^{-1} for *p*pR and pR_K, respectively. These frequencies are close to those of BR (2506 and 2466 cm^{-1} for BR and BR_K, respectively), suggesting the interaction of Thr79 and Asp75 in *p*pR is similar to that of Thr89 and Asp85 in BR. On the other hand, a frequency shift higher by 6−8 cm^{-1} in *p*pR than in BR indicates a weaker interaction between Thr79 and Asp75 in *p*pR. This may be reasonable because the interaction between the Schiff base and an oxygen of Asp75 in *p*pR (Figure 1) is stronger than the corresponding one in BR, so the other oxygen of Asp75 that interacts with Thr79 is less negatively charged in *p*pR.

Clear contrast between *p*pR and BR was seen in the 2300−2000 cm^{-1} region. The N−D stretch of the Schiff base and the O−D stretch of water molecules appear in separate frequency regions in *p*pR (Figure 4) (*8*, *16*), while they appear in the same frequency region in BR (*8*, *12*). This can be correlated with the structural difference in the pentagonal cluster in the Schiff base region, where it is much distorted in *p*pR (Figure 1). Hayashi and Ohmine reported the importance of the coupling of the vibrational modes of the Schiff base N−D and water O−D stretches in their quantum mechanical/molecular mechanical (QM/MM) calculation for BR (*32*). The hydrogen bond from Arg82 to the pentagonal cluster structure in BR, not for Arg72 in *p*pR (Figure 1), would be an important component. The structural difference in the pentagonal cluster may also be related to the 70 nm difference in the absorption spectra of *p*pR and BR. Normal-mode analysis on the basis of such QM/MM calculation is necessary to evaluate the vibrational characters in *p*pR.

Despite these detailed differences, the proton transfer reaction takes place from the Schiff base to Asp75 in *p*pR at the M state as well as for BR (*33*). Similar primary reactions accompanying K formation may be correlated with the same reaction. Namely, K formation accompanies the weakened hydrogen bond of the Schiff base, the weakened hydrogen bond of the bridged water molecules (*16*), and the strengthened hydrogen bond of Thr79 with Asp75 in *p*pR (Thr89 with Asp85 in BR). Recently, we proposed a model of the proton transfer mechanism from the Schiff base to Asp85 in BR (*11*). According to the hydration switch model, the hydrogen bond of the bridged water molecule between the Schiff base and Asp85 is switched from Asp85 in L to Asp212 in M, so proton transfer takes place simultaneously (*11*). Similar primary reactions in *p*pR suggest the similar mechanism of proton transfer from the Schiff base to Asp75 upon M formation, which should be shown experimentally in the future.

ACKNOWLEDGMENT

We thank Dr. M. Iwamoto and F. Urazono for helping in sample preparation.

REFERENCES

1. Kamo, N., Shimono, K., Iwamoto, M., and Sudo, Y. (2001) *Biochemistry (Moscow) 66*, 1277−1282.
2. Sasaki, J., and Spudich, J. L. (2000) *Biochim. Biophys. Acta 1460*, 230−239.
3. Spudich, J. L., and Lanyi, J. K. (1996) *Curr. Opin. Cell Biol. 8*, 452−457.
4. Kandori, H., Tomioka, H., and Sasabe, H. (2002) *J. Phys. Chem. A 106*, 2091−2095.
5. Lutz, I., Sieg, A., Wegener, A. A., Engelhard, M., Boche, I., Otsuka, M., Oesterhelt, D., Wachtveitl, J., and Zinth, W. (2001) *Proc. Natl. Acad. Sci. U.S.A. 98*, 962−967.
6. Luecke, H., Schobert, B., Lanyi, J. K., Spudich, E. N., and Spudich, J. L. (2001) *Science 293*, 1499−1503.
7. Royant, A., Nollert, P., Edman, K., Neutze, R., Landau, E. M., Pebay-Peyroula, E., and Navarro, J. (2001) *Proc. Natl. Acad. Sci. U.S.A. 98*, 10131−10136.
8. Furutani, Y., and Kandori, H. (2002) *Mol. Membr. Biol. 19*, 257−265.
9. Kandori, H. (2000) *Biochim. Biophys. Acta 1460*, 176−190.
10. Kandori, H., and Shichida, Y. (2000) *J. Am. Chem. Soc. 122*, 11745−11746.
11. Tanimoto, T., Furutani, Y., and Kandori, H. (2003) *Biochemistry 42*, 2300−2306.
12. Kandori, H., Belenky, M., and Herzfeld, J. (2002) *Biochemistry 41*, 6026−6031.
13. Kandori, H., Kinoshita, N., Yamazaki, Y., Maeda, A., Shichida, Y., Needleman, R., Lanyi, J. K., Bizounok, M., Herzfeld, J., Raap, J., and Lugtenburg, J. (1999) *Biochemistry 38*, 9676−9683.
14. Kandori, H., Kinoshita, N., Yamazaki, Y., Maeda, A., Shichida, Y., Needleman, R., Lanyi, J. K., Bizounok, M., Herzfeld, J., Raap, J., and Lugtenburg, J. (2000) *Proc. Natl. Acad. Sci. U.S.A. 97*, 4643−4648.
15. Kandori, H., Yamazaki, Y., Shichida, Y., Raap, J., Lugtenburg, J., Belenky, M., and Herzfeld, J. (2001) *Proc. Natl. Acad. Sci. U.S.A. 98*, 1571−1576.
16. Kandori, H., Furutani, Y., Shimono, K., Shichida, Y., and Kamo, N. (2001) *Biochemistry 40*, 15693−15698.

17. Shimono, K., Iwamoto, M., Sumi, M., and Kamo, N. (1997) *FEBS Lett. 420*, 54−56.
18. Tanaka, T., Ames, J. B., Kainosho, M., Stryer, L., and Ikura, M. (1998) *J. Biomol. NMR 11*, 135−152.
19. Kandori, H., Shimono, K., Sudo, Y., Iwamoto, M., Shichida, Y., and Kamo, N. (2001) *Biochemistry 40*, 9238−9246.
20. Klare, J. P., Schmies, G., Chizhov, I., Shimono, K., Kamo, N., and Engelhard, M. (2002) *Biophys. J. 82*, 2156−2164.
21. Arakawa, T., Shimono, K., Yamaguchi, S., Tuzi, S., Sudo, Y., Kamo, N., and Saitô, H. (2003) *FEBS Lett. 536*, 237−240.
22. Kandori, H., Shimono, K., Shichida, Y., and Kamo, N. (2002) *Biochemistry 41*, 4554−4559.
23. Gellini, C., Lüttenberg, B., Sydor, J., Engelhard, M., and Hildebrandt, P. (2000) *FEBS Lett. 472*, 263−266.
24. Aton, B., Doukas, A. G., Callender, R. H., Dinur, U., and Honig, B. (1980) *Biophys. J. 29*, 79−94.
25. Rodman-Gilson, H. S., Honig, B., Croteau, A., Zarrilli, G., and Nakanishi, K. (1988) *Biophys. J. 53*, 261−269.
26. Baasov, T., Friedman, N., and Sheves, M. (1987) *Biochemistry 26*, 3210−3217.
27. Edman, K., Nollert, P., Royant, A., Belrhali, H., Pebay-Peyroula, E., Hajdu, J., Neutze, R., and Landau, E. M. (1999) *Nature 401*, 822−826.
28. Schobert, B., Cupp-Vickery, J., Hornak, V., Smith, S. O., and Lanyi, J. K. (2002) *J. Mol. Biol. 321*, 715−726.
29. Matsui, Y., Sakai, K., Murakami, M., Shiro, Y., Adachi, S., Okumura, H., and Kouyama, T. (2002) *J. Mol. Biol. 324*, 469−481.
30. Edman, K., Royant, A., Nollert, P., Maxwell, C. A., Pebay-Peyroula, E., Navarro, J., Neutze, R., and Landau, E. M. (2002) *Structure 10*, 473−482.
31. Nagata, T., Oura, T., Terakita, A., Kandori, H., and Shichida, Y. (2002) *J. Phys. Chem. A 106*, 1969−1975.
32. Hayashi, S., and Ohmine, I. (2000) *J. Phys. Chem. B 104*, 10678−10691.
33. Furutani, Y., Iwamoto, M., Shimono, K., Kamo, N., and Kandori, H. (2002) *Biophys. J. 83*, 3482−3489.
34. Furutani, Y., Sudo, Y., Kamo, N., and Kandori, H. (2003) *Biochemistry 42*, 4837−4842.

BI034284M